


# XRCC1 counteracts poly(ADP ribose)polymerase (PARP) poisons, olaparib and talazoparib, and a clinical alkylating agent, temozolomide, by promoting the removal of trapped PARP1 from broken DNA

Kouji Hirota<sup>1,2</sup>  | Masato Ooka<sup>2,6</sup> | Naoto Shimizu<sup>1</sup> | Kousei Yamada<sup>1</sup> | Masataka Tsuda<sup>1,3</sup> | Mahmoud Abdelghany Ibrahim<sup>1</sup> | Shintaro Yamada<sup>1</sup> | Hiroyuki Sasanuma<sup>1</sup> | Mitsuko Masutani<sup>4</sup> | Shunichi Takeda<sup>5</sup>

<sup>1</sup>Department of Radiation Genetics, Graduate School of Medicine, Kyoto University, Kyoto, Japan

<sup>2</sup>Department of Chemistry, Graduate School of Science, Tokyo Metropolitan University, Tokyo, Japan

<sup>3</sup>Department of Mathematical and Life Sciences, Graduate School of Science, Hiroshima University, Hiroshima, Japan

<sup>4</sup>Department of Molecular and Genomic Biomedicine, CBMM, Nagasaki University Graduate School of Biomedical Sciences, Nagasaki, Japan

<sup>5</sup>Shenzhen University School of Medicine, Shenzhen, Guangdong, China

<sup>6</sup>Division of Pre-Clinical Innovation, National Center for Advancing Translational Sciences, National Institutes of Health, Bethesda, Maryland, USA

## Correspondence

Kouji Hirota, Department of Chemistry, Graduate School of Science, Tokyo Metropolitan University, Tokyo, Japan  
Email: khirota@tmu.ac.jp

Shunichi Takeda, Shenzhen University School of Medicine, Shenzhen, Guangdong 518060, China.  
Email: stakeda@szu.edu.cn

## Funding information

JSPS KAKENHI, Grant/Award Numbers: JP20H04337, JP19KK0210, JP16H01314, and JP16H06306; Takeda Science Foundation; Yamada Science Foundation, JSPS KAKENHI; JSPS Core-to-Core Program, A. Advanced Research Networks

**Communicated by:** Akira Shinohara

## Abstract

Base excision repair (BER) removes damaged bases by generating single-strand breaks (SSBs), gap-filling by DNA polymerase  $\beta$  (POL $\beta$ ), and resealing SSBs. A base-damaging agent, methyl methanesulfonate (MMS) is widely used to study BER. BER increases cellular tolerance to MMS, anti-cancer base-damaging drugs, temozolomide, carmustine, and lomustine, and to clinical poly(ADP ribose)polymerase (PARP) poisons, olaparib and talazoparib. The poisons stabilize PARP1/SSB complexes, inhibiting access of BER factors to SSBs. PARP1 and XRCC1 collaboratively promote SSB resealing by recruiting POL $\beta$  to SSBs, but *XRCC1*<sup>-/-</sup> cells are much more sensitive to MMS than *PARP1*<sup>-/-</sup> cells. We recently report that the PARP1 loss in *XRCC1*<sup>-/-</sup> cells restores their MMS tolerance and conclude that XPCC1 facilitates the release of PARP1 from SSBs by maintaining its autoPARylation. We here show that the PARP1 loss in *XRCC1*<sup>-/-</sup> cells also restores their tolerance to the three anti-cancer base-damaging drugs, although they and MMS induce different sets of base damage. We reveal the synthetic lethality of the *XRCC1*<sup>-/-</sup> mutation, but not *POL $\beta$* <sup>-/-</sup>, with olaparib and talazoparib, indicating that XRCC1 is a unique BER factor in suppressing toxic PARP1/SSB complex and can suppress even when PARP1

catalysis is inhibited. In conclusion, XRCC1 suppresses the PARP1/SSB complex via PARP1 catalysis-dependent and independent mechanisms.

#### KEYWORDS

carmustine, lomustine, olaparib, PARP poison, PARP1, talazoparib, temozolomide, XRCC1

## 1 | INTRODUCTION

Glioblastoma multiform (GBM) is the most common primary malignant brain tumor in adults. Chemotherapeutic agents, temozolomide (TMZ), carmustine, and lomustine, are alkylating agents, cross the blood–brain barrier, and are the standard chemotherapy for GBMs (Desai et al., 2019). The TMZ-mediated methylation of bases plays a crucial role in suppressing the proliferation of glioma cells. This view is supported by the data that O-6-methylguanine DNA methyltransferase counteracts the cytotoxic effect of these alkylating agents by removing methyl groups from the O(6)-alkylguanine and other methylated moieties of genomic DNA (Esteller et al., 2000; Kaina et al., 2007; Stupp et al., 2019; Yu et al., 2019). Derivatives of nitrosourea, carmustine and lomustine, seem to kill malignant cells mainly by chloroethylating O-6-guanine (Penketh et al., 2000). The three alkylating agents generate different sets of multiple base lesions in vivo (Figure S1). Base excision repair (BER) removes various base lesions and significantly increases the resistance of malignant tumors to the three clinical alkylating agents (reviewed in Thomas et al., 2017; Kaina & Christmann, 2019). Previous studies examined the molecular mechanism of BER using methyl methanesulfonate (MMS) as a model alkylating agent (Demin et al., 2021). However, it is unclear whether the mechanism for MMS-induced damage repair is relevant to the repair of DNA lesions induced by clinical alkylating agents for treating GBM.

A large number of base damages occur daily in every cell (Figure S2a), and BER is essential for the viability of cells (Barnes & Lindahl, 2004; Tubbs & Nussenzweig, 2017). BER initiates by hydrolyzing damaged bases, forming abasic (AP) sites (Figure S2b). AP-endonuclease incises DNA 5' to the AP sites, generating single-strand breaks (SSBs) with an OH group at the 3' end and a deoxyribose phosphate group at the 5' end (5'-dRP) (Figure S2c) (Doetsch et al., 1986; Doetsch & Cunningham, 1990). SSB repair is a subpathway of BER and starts with the physical interaction of PARP1 with SSBs (Figure S2d), leading to the robust activation of PARP1 (Figures S2e and S3a) (Cistulli et al., 2004; Okano et al., 2003). PARP1 PARylates itself (auto-PARylation) and chromatin proteins using NAD<sup>+</sup> as a substrate (Figure S2e) (Satoh & Lindahl, 1992), thereby recruiting PAR-interacting proteins, ALC1/CHD1L (Ahel et al., 2009; Tsuda, Cho,

et al., 2017) and X-ray repair cross-complementing 1 (XRCC1) (Figure S2f) (Caldecott et al., 1995; Caldecott et al., 1996; El-Khamisy et al., 2003), to SSBs (reviewed in Caldecott, 2014). The auto-PARylation of PARP1 promotes its release from unrepaired SSBs (Figures S2f and S3b), allowing downstream SSB repair enzymes to access the SSBs (Figure S2g,h) (Satoh & Lindahl, 1992). XRCC1 recruited to SSBs provides docking sites for the downstream SSB repair factors, aprataxin, LIG3, PNKP, and polymerase  $\beta$  (POL $\beta$ ) (Ali et al., 2009; Caldecott, 2003; Caldecott, 2008; Caldecott et al., 1994; Caldecott et al., 1996; Cuneo & London, 2010; Horton et al., 2008; Iles et al., 2007; Kubota et al., 1996; Marintchev et al., 1999) (reviewed in Caldecott, 2020). While core factors of BER are conserved between lower and higher eukaryotes, mammalian cells evolve accessory proteins, such as PARP1 and XRCC1 (Demin et al., 2021). The critical role of XRCC1 in BER is supported by the embryonic lethality of XRCC1-deficient mice (Tebbs et al., 1999; Tebbs et al., 2003). The genetic deletion of PARP1 partially rescues cerebellar neurodegeneration in neuron-specific XRCC1-deficient mice by preventing the depletion of NAD<sup>+</sup> in neurons (Hoch et al., 2017). We recently showed that the inactivation of PARP1 rescues the hypersensitivity of XRCC1-deficient cells to an alkylating agent, MMS (Demin et al., 2021). However, it remains unclear whether this inactivation also reverses cells deficient in BER factors other than XRCC1. Another unsolved question is whether the inactivation of PARP1 reverses the sensitivity of BER mutants to anti-cancer alkylating drugs.

Olaparib and talazoparib selectively kill the malignant tumors carrying mutations in homologous recombination factors such as BRCA1 and BRCA2 (Bryant et al., 2005; Farmer et al., 2005; Fong et al., 2009; Murai et al., 2014; Shen et al., 2013; Yap et al., 2019). Olaparib and talazoparib are considerably more cytotoxic than the loss of PARP1 (Figure S3c,d) and the PARP catalytic inhibitor (Figure S3e,f), and this more potent cytotoxic effect is due to their PARP poison activity, where they stabilize the PARP1/SSB complex that blocks the access of POL $\beta$  and DNA-ligases to unrepaired SSBs (Figure S3g,h) (Murai et al., 2012; Murai et al., 2014). We hereafter call the catalytic inhibitor when a drug kills *wild-type* and *PARP1*<sup>-/-</sup> cells to the same extent, like veliparib, and define the PARP poison as the drug whose cytotoxicity to *wild-type* is greater than to *PARP1*<sup>-/-</sup>

(Horton & Wilson, 2013; Murai et al., 2012; Prasad et al., 2014; Ray Chaudhuri & Nussenzweig, 2017). The PARP poison activity (Figure S3g,h), but not the catalytic inhibition of PARP1 (Figure S3e,f), accounts for the anti-cancer effect of olaparib and talazoparib (Horton & Wilson, 2013; Murai et al., 2012; Prasad et al., 2014; Ray Chaudhuri & Nussenzweig, 2017). As expected, the PARP poison sensitizes BER-deficient cells, including cells deficient in ALC1, POL $\beta$ , and XRCC1 (Blessing et al., 2020; Hewitt et al., 2021; Horton et al., 2014; Juhász et al., 2020; Verma et al., 2021). We recently showed that a PARP1 inhibitor (KU0058948) significantly increased the number of MMS-induced PARP1/SSB complexes in *wild-type* cells but not XRCC1-deficient cells (Demin et al., 2021). However, it is unclear whether clinical PARP poisons have the same effect on XRCC1-deficient cells as KU0058948, whose poison activity is poorly characterized.

We disrupted the *PARP1* gene in *ALC1*<sup>-/-</sup>, *POL $\beta$* <sup>-/-</sup>, and *XRCC1*<sup>-/-</sup> cells. The disruption in *XRCC1*<sup>-/-</sup> cells, but not *ALC1*<sup>-/-</sup> or *POL $\beta$* <sup>-/-</sup> cells, reversed their tolerance to TMZ, and the resulting *PARP1*<sup>-/-</sup>/*XRCC1*<sup>-/-</sup> cells showed only modest sensitivity to TMZ. Likewise, the loss of PARP1 reversed the hypersensitivity of *XRCC1*<sup>-/-</sup> cells to carmustine and lomustine. We, therefore, conclude that XRCC1 suppresses the toxic PARP1/SSB complexes formation during BER of DNA damage generated by the three clinical alkylating agents as well as by MMS (Demin et al., 2021). We showed that ALC1 and POL $\beta$  do not share this function. *XRCC1*<sup>-/-</sup> cells displayed over two orders magnitudes higher sensitivities to olaparib and talazoparib than *wild-type*, *ALC1*<sup>-/-</sup>, and *POL $\beta$* <sup>-/-</sup> cells, indicating that XRCC1 also prevents PARP1 ‘trap’ at SSBs even when the catalytic activity of PARP1 is inhibited. We previously proposed that XRCC1 prevents the PARP1 trap by maintaining auto-PARYlation (Demin et al., 2021). Thus, XRCC1 inhibits the toxic PARP1/SSB complexes formation through the PARP1 catalytic activity-independent mechanism and dependent one. In conclusion, toxic PARP1/SSB complexes frequently form during BER of clinical alkylating agents, and XRCC1 suppresses the toxic effect of PARP1 and counteracts clinical PARP poisons.

## 2 | RESULTS

### 2.1 | *XRCC1*<sup>-/-</sup> cells show higher sensitivity to the alkylating agent in comparison with *ALC1*<sup>-/-</sup>, *PARP1*<sup>-/-</sup>, and *POL $\beta$* <sup>-/-</sup> cells

We examined the sensitivity profile of a simple alkylating agent, MMS, by mining the CRISPR-Cas9 screen data of human retinal pigment epithelial (RPE)

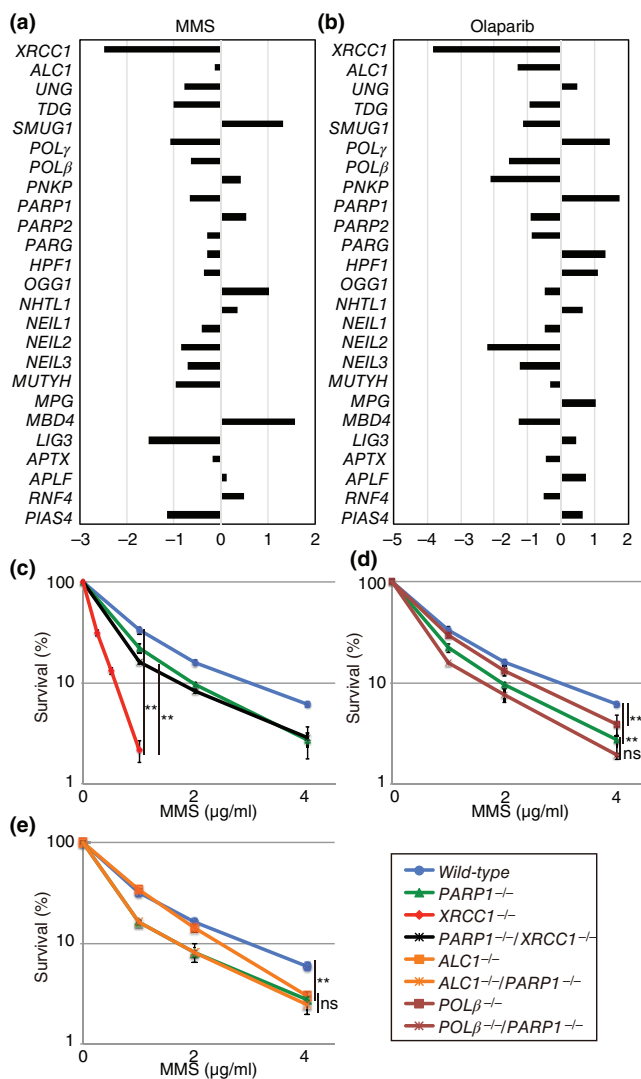


**FIGURE 1** *XRCC1*<sup>-/-</sup> cells show higher sensitivity to MMS and olaparib than *ALC1*<sup>-/-</sup>, *PARP1*<sup>-/-</sup>, and *POL $\beta$* <sup>-/-</sup> cells. (a,b) Sensitivity profiles of MMS (a) and olaparib (b) in the selected RPE cells deficient in individual BER and PARP-related factors were calculated by mining an open database (Olivieri et al., 2020). The relative sensitivity of each cell compared to *wild-type* RPE cells was scored as log<sub>2</sub> (LD20% in indicated mutant cells)/(LD20% in *wild-type* cells). LD20% represents drug concentrations that reduce cell survival to 20% relative to that of untreated cells. Negative (left) and positive (right) scores indicate that the indicated gene-disrupted cells are sensitive and resistant to MMS (a) and olaparib (b), respectively. (c-e) The loss of PARP1 reversed the hypersensitivity to MMS in *XRCC1*<sup>-/-</sup> cells, but not in *ALC1*<sup>-/-</sup> or *POL $\beta$* <sup>-/-</sup> cells. TK6 cells carrying the indicated genotypes were treated with MMS for 72 h. The drug dose is displayed on the x-axis on a linear scale, while the percentage of cell survival is displayed on the y-axis on a logarithmic scale. Error bars represent the SD from three independent experiments. The *p*-value was calculated by Student's *t*-test (\**p* < 0.05). BER, base excision repair; MMS, methyl methanesulfonate; ns, not significant; PARP, poly(ADP ribose) polymerase; RPE cells, retinal pigment epithelial cells

cells (Olivieri et al., 2020). We examined cells deficient in SSB repair factors, including ALC1/CHD1L, APTX, LIG3, PARP1, PARP2, PNKP, POL $\beta$ , and XRCC1. The loss of XRCC1 causes the most pronounced increases in the sensitivity of both MMS (Figure 1a) and olaparib (Figure 1b). Although PARP1 acts upstream of XRCC1 in SSB repair, the loss of PARP1 increases MMS sensitivity by several times less than the loss of XRCC1. The loss of PARP2 does not increase MMS sensitivity (Figure 1a). We examined the MMS sensitivity of human TK6 B-lymphoblastoid cells, where O-6-methylguanine DNA methyltransferase is inactive (Danam et al., 2005; Zhang et al., 1995) (Figure 1c). The list of the analyzed gene-disrupted clones is shown in Table S1 and Figures S4 and S5 (Saha et al., 2020; Tsuda, Cho, et al., 2017). Consistent with Figure 1a, *XRCC1*<sup>-/-</sup> cells exhibited a few times higher MMS sensitivity than *ALC1*<sup>-/-</sup>, *PARP1*<sup>-/-</sup>, and *POL $\beta$* <sup>-/-</sup> cells (Figure 1c).

To elucidate the functional interaction between PARP1 and XRCC1, we generated *PARP1*<sup>-/-</sup>/*XRCC1*<sup>-/-</sup> TK6 cells. Remarkably, the loss of PARP1 reversed the MMS hypersensitivity of *XRCC1*<sup>-/-</sup> cells to that of *PARP1*<sup>-/-</sup> cells (Figure 1c). By contrast, the loss of PARP1 reversed the MMS hypersensitivity of neither *ALC1*<sup>-/-</sup> nor *POL $\beta$* <sup>-/-</sup> cells (Figure 1d,e). The data suggest that XRCC1 may have a previously unappreciated role in BER, suppressing the toxic effect of PARP1 on BER.

## 2.2 | Loss of PARP1 in *XRCC1*<sup>-/-</sup> cells reverses their hypersensitivity to TMZ

We next investigated the sensitivity to TMZ. *XRCC1*<sup>-/-</sup> cells showed a few times higher sensitivity than *ALC1*<sup>-/-</sup>, *PARP1*<sup>-/-</sup>, and *POL $\beta$* <sup>-/-</sup> cells (Figure 2a), and the loss of PARP1 in *XRCC1*<sup>-/-</sup> cells reversed their hypersensitivity (Figure 2b, left). We prepared *PARP1*<sup>-/-</sup>, *XRCC1*<sup>-/-</sup>, and *PARP1*<sup>-/-</sup>/*XRCC1*<sup>-/-</sup> cells from MCF-7 human breast cancer cells (Table S1 and Figure S5). The sensitivity of *XRCC1*<sup>-/-</sup> cells to TMZ was considerably higher than that of *PARP1*<sup>-/-</sup> cells (Figure 2b, right), and this hypersensitivity was reversed by the ectopic expression of *XRCC1* cDNA (Figure S6a). Like the B lymphoblastoid cell, the loss of PARP1 in *XRCC1*<sup>-/-</sup> cells reversed their TMZ hypersensitivity to the level of *PARP1*<sup>-/-</sup> cells (Figure 2b, right). In summary, *PARP1*<sup>-/-</sup> and *PARP1*<sup>-/-</sup>/*XRCC1*<sup>-/-</sup> cells showed very similar increases in the sensitivity to TMZ compared to *wild-type* cells. This result agrees with the previously identified collaboration between PARP1 and XRCC1 in SSB repair (Ali et al., 2009; Caldecott, 2003; Caldecott, 2008; Caldecott et al., 1994; Caldecott et al., 1996; Cuneo &

London, 2010; Horton et al., 2008; Iles et al., 2007; Kubota et al., 1996; Marintchev et al., 1999). More importantly, the much higher sensitivity of *XRCC1*<sup>-/-</sup> cells to TMZ compared with *PARP1*<sup>-/-</sup>/*XRCC1*<sup>-/-</sup> cells suggests that PARP1 can interfere with BER of TMZ-induced lesion, and XRCC1 counteracts against this interference.

We also examined the cellular sensitivity of *XRCC1*<sup>-/-</sup>, *PARP1*<sup>-/-</sup>, and *PARP1*<sup>-/-</sup>/*XRCC1*<sup>-/-</sup> cells to carmustine and lomustine, alkylating agents for anti-cancer therapy (Figure S7). *XRCC1*<sup>-/-</sup> cells exhibited higher sensitivity to both carmustine and lomustine than *wild-type* and *PARP1*<sup>-/-</sup> cells, and loss of PARP1 in *XRCC1*<sup>-/-</sup> MCF-7 cells reversed their sensitivity (Figure S7). These results suggest that XRCC1 suppresses the toxic effect of PARP1 on BER of DNA lesions induced by three clinically relevant DNA alkylating reagents, TMZ, carmustine, and lomustine.

## 2.3 | Delayed SSB repair causes the hypersensitivity of *XRCC1*<sup>-/-</sup> cells to TMZ

To measure BER kinetics, we measured the amounts of SSBs, BER intermediates after a pulse exposure to TMZ for 60 min, using the alkaline comet assay. Consistent with the TMZ sensitivity, while *XRCC1*<sup>-/-</sup> cells showed the prominent accumulation of SSBs upon the pulse-exposure, the loss of PARP1 in *XRCC1*<sup>-/-</sup> cells suppressed this accumulation (Figure 3a and S8a). The result suggests that XRCC1 protects SSB repair from the inhibitory effect of PARP1.

To accurately examine the SSB repair kinetics, we pulse-exposed cells to H<sub>2</sub>O<sub>2</sub> on ice to induce SSBs, then removed H<sub>2</sub>O<sub>2</sub> and incubated cells at 37°C, monitoring SSB repair kinetics over time (Figure 3b and S8b) (Breslin et al., 2006). Note that while the exposure to H<sub>2</sub>O<sub>2</sub> on ice inhibits SSB repair, the exposure to TMZ simultaneously induces DNA damage and its repair reaction, making it impossible to measure the SSB repair kinetics accurately. The pulse-exposure to H<sub>2</sub>O<sub>2</sub> induced indistinguishable levels of SSBs in all tested genotypes. At 5 min incubation at 37°C, the length of tails in *wild-type* cells decreased by over 80%, while that in *XRCC1*<sup>-/-</sup> cells decreased only 25% (Figures 3b and S8b), indicating a significant delay in SSB repair in the absence of XRCC1. The loss of PARP1 in *XRCC1*<sup>-/-</sup> cells restored the SSB repair to the level of *PARP1*<sup>-/-</sup> cells. We, therefore, concluded that PARP1 can block physiological SSB repair, and XRCC1 suppresses the toxic effect of PARP1 on SSB repair. Taken together, the hypersensitivity of *XRCC1*<sup>-/-</sup> cells to TMZ is attributable to the toxic effect of PARP1 on SSB



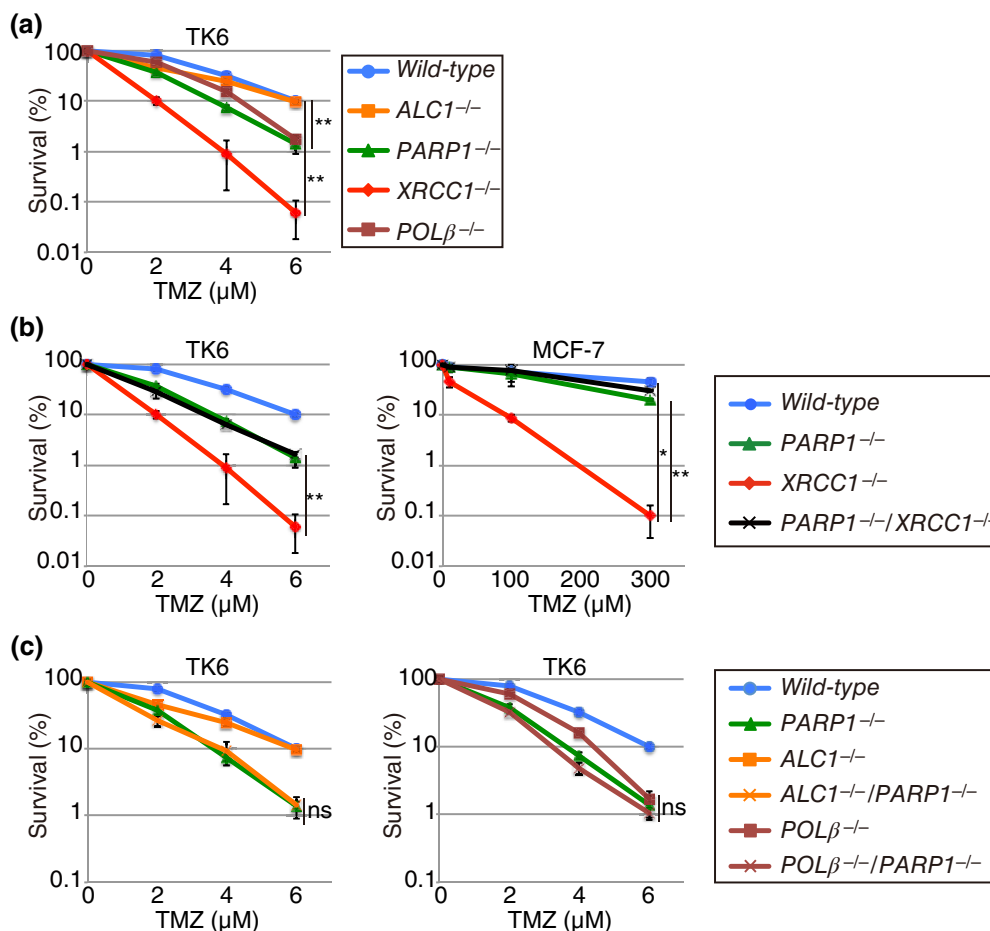


**FIGURE 2** The hypersensitivity of  $XRCC1^{-/-}$  cells to TMZ is rescued by the loss of PARP1. (a–c) The indicated TK6 cells were assessed for sensitivity to temozolomide (TMZ). The degree of the hypersensitivity to TMZ was compared in  $ALC1^{-/-}$ ,  $PARP1^{-/-}$ ,  $POL\beta^{-/-}$ , and  $XRCC1^{-/-}$  cells (a). The genetic relationships between  $PARP1$  and  $XRCC1$  were examined (b). The genetic relationships between  $PARP1$  and  $ALC1$  or  $POL\beta$  were examined (c). TK6 cells with the indicated genotype were treated with TMZ for 24 h, then cultured in a drug-free methylcellulose medium for 14 days. MCF-7 cells with the indicated genotype were treated with indicated alkylating agent for 24 h, then cultured in a drug-free medium for 14 days. Cell viability was assessed as described in Materials and Methods. The drug dose is displayed on the x-axis on a linear scale, while the percentage of cell survival is displayed on the y-axis on a logarithmic scale. Error bars represent the SD from three independent experiments. The  $p$ -value was calculated by Student's  $t$ -test (\* $p < 0.05$ , \*\* $p < 0.01$ ). ns, not significant; PARP, poly(ADP ribose)polymerase; TMZ, temozolomide

repair, similar to the hypersensitivity of  $XRCC1^{-/-}$  cells to MMS (Demin et al., 2021).

## 2.4 | XRCC1 prevents the accumulation of toxic PARP1/SSB complex

The loss of XRCC1 causes the accumulation of PARP1 'trapped' at unrepaired SSBs in the chromatin-bound fraction (Murai et al., 2012; Murai et al., 2014) following exposure to MMS (Demin et al., 2021). We examined the effect of TMZ on PARP1 trapping. TMZ induced a faint PARP1 signal ( $\sim 10\%$  increase at 1 h after TMZ treatment) in the chromatin fraction in *wild-type* TK6 cells (Figure 4). In contrast with *wild-type* cells, TMZ alone induced the prominent accumulation of trapped PARP1

in  $XRCC1^{-/-}$  TK6 and MCF-7 cells (Figures 4 and S9). We conclude that XRCC1 prevents the trapping of PARP1 at TMZ-induced SSBs.

## 2.5 | XRCC1 avoids quick depletion of cellular $\text{NAD}^+$ during BER

The auto-PARylation of PARP1 promotes its release from unrepaired SSBs (Figures S2e,f and S3a,b) (Satoh & Lindahl, 1992), and XRCC1 prevents toxic PARP1/SSB complex by maintaining auto-PARylation level during MMS treatment (Demin et al., 2021). We then asked whether this is also the case in the repair of TMZ-induced DNA damages. We assessed the extent of auto-PARylation, its chain length, and/or branching

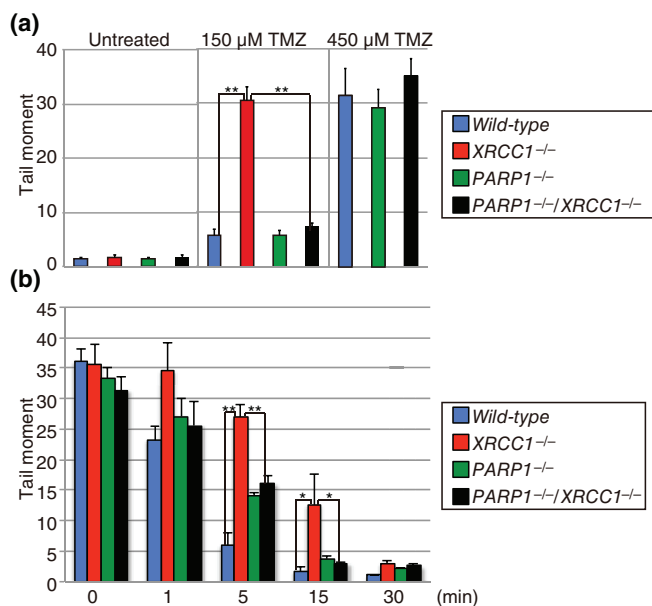


**FIGURE 3** XRCC1<sup>-/-</sup> cells but not PARP1<sup>-/-</sup>/XRCC1<sup>-/-</sup> cells show delayed BER kinetics upon TMZ treatment. (a) Alkaline-comet assay to measure the number of unrepaired SSBs after TMZ addition. Indicated cells were treated with TMZ (0, 150, or 450 μM) for 1 h. (b) Alkaline-comet assay to measure the repair kinetics of SSBs. The indicated TK6 cells were exposed to H<sub>2</sub>O<sub>2</sub> (80 μM) on ice for 30 min, then released into a drug-free, prewarmed culture medium for the indicated times. The median of tail moments for 50 nuclei was measured three times in independent experiments. The means of the tail moments are displayed on the y-axis on a linear scale. Error bars represent SD from three independent experiments. Each data set was presented in Figure S8. The *p*-value was calculated by Student's *t*-test (\**p* < 0.05, \*\**p* < 0.01). BER, base excision repair; SSBs, single-strand breaks; TMZ, temozolomide

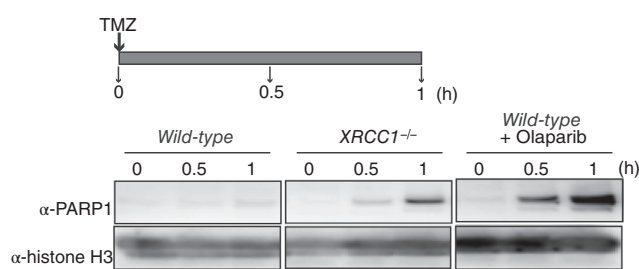


**FIGURE 4** Role of XRCC1 in the resolution of PARP1/DNA complexes. Western blot of chromatin-bound fractions prepared from human TK6 clones. The indicated cells were treated with 1 mM TMZ under the presence or absence of olaparib (10 μM) for indicated durations. Blots were probed with the indicated antibodies. Histone H3 was probed as a loading control. PARP1, poly(ADP ribose)polymerase 1; TMZ, temozolomide

complexity over time after exposing cells to TMZ using an anti-poly(ADP-ribose)-specific antibody (Figure 5a). We evaluated the extent of PARP1 auto-PARylation by

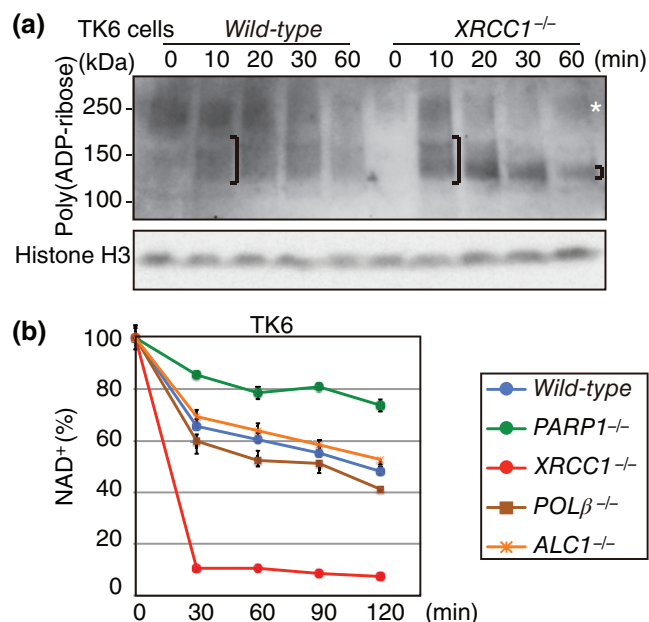


**FIGURE 5** XRCC1 maintains PARP1 auto-PARylation levels by avoiding rapid depletion of cellular NAD<sup>+</sup>. (a) PARP1 auto-PARylation detected by anti-poly(ADP-ribose)-specific antibody in *wild-type* and XRCC1<sup>-/-</sup> TK6 cells. Cells were treated with 1 mM TMZ for the indicated time. Histone H3 was probed as a loading control. Open parentheses represent the signal of PARP1 auto-PARylation. White asterisk indicating signals of ~250 kDa PARylated molecules do not represent PARylated PARP1 as PARP1<sup>-/-</sup> cells also exhibited this signal (Figure S10). (b) Rapid depletion of cellular NAD<sup>+</sup> in XRCC1<sup>-/-</sup> cells. Indicated TK6 cells were treated with TMZ (1 mM) for the indicated time. Error bars represent the SD from three independent measurements. PARP1, poly(ADP ribose)polymerase 1; TMZ, temozolomide

detecting the retarded electrophoretic mobility of poly-ribosylated proteins. By comparing *wild-type* and PARP1<sup>-/-</sup> TK6 cells, we found that slow migrating signal around 250 kb is non-specific signal (Figures S10 and 5a, indicated by asterisk). The addition of TMZ induced slow-migrating signals, ~150 kDa, in *wild-type* and XRCC1<sup>-/-</sup> TK6 cells to a similar extent at an initial time point, 10 min post-TMZ treatment, indicating the initiation of auto-PARylation in the absence of XRCC1 (Figure 5a, wide-open parentheses). Constant PARylated PARP1 signals were detectable over 60 min in *wild-type* cells (Figure 5a, wide-open parentheses). By contrast, the intensity of PARylated PARP1 signals significantly dropped at 20 min in XRCC1<sup>-/-</sup> cells with a band corresponding to the molecular size of PARP1, 116 kDa, increasing in its relative intensity at 20–60 min (Figure 5a, small open parenthesis). Thus, TMZ-induced auto-PARylation rapidly dropped in the absence of XRCC1, as seen in MMS-treated XRCC1<sup>-/-</sup> cells (Demin et al., 2021).

The absence of XRCC1 causes the excessive catalysis of PARP1, depletes  $\text{NAD}^+$ , and reduces auto-PARYlation in MMS-treated cells (Demin et al., 2021). We then measured the cellular concentration of  $\text{NAD}^+$  during exposure cells to TMZ (Figure 5b). The concentration of  $\text{NAD}^+$  gradually reduced over time in *wild-type*, *ALC1*<sup>-/-</sup>, and *POLβ*<sup>-/-</sup> cells in a very similar manner (Figure 5b). As expected, *PARP1*<sup>-/-</sup> cells showed only a modest decrease in the  $\text{NAD}^+$  concentration. Strikingly, the concentrations of  $\text{NAD}^+$  in *XRCC1*<sup>-/-</sup> cells were reduced to a basal level at 30 min (Figure 5b), more rapid when compared with MMS-treated *XRCC1*<sup>-/-</sup> cells (Demin et al., 2021). These data indicate that XRCC1 prevents the rapid depletion of cellular  $\text{NAD}^+$ , thereby maintaining the auto-PARYlation and facilitating the release of PARP1 from SSBs. Collectively, XRCC1 inhibits the prolonged formation of toxic PARP1/SSB complex by maintaining the auto-PARYlation.

## 2.6 | Synthetic lethality of clinical PARP poisons in *XRCC1*<sup>-/-</sup> cells

We investigated whether or not clinical PARP poisons were synthetic lethal to XRCC1-deficient cells. The loss of XRCC1 decreased the plating efficiency of TK6 and MCF-7 cells only by 85% and 38%, respectively. A clinically relevant concentration of olaparib, 0.1  $\mu\text{M}$  (Sun et al., 2018) had no detectable effect on the viability of *wild-type*, *ALC1*<sup>-/-</sup>, and *POLβ*<sup>-/-</sup> cells (Figures 6a,b and S11). By sharp contrast, 0.1  $\mu\text{M}$  olaparib reduced the viability of *XRCC1*<sup>-/-</sup> by more than 10 times (Figure 6b). Similarly, *XRCC1*<sup>-/-</sup> MCF-7 cells exhibited 100 times higher sensitivity than *wild-type* as judged by LD50%, the dose of olaparib reduces the viability by 50% relative to nontreated cells (Figure 6c,d). The ectopic expression of XRCC1 reversed the olaparib sensitivity of *XRCC1*<sup>-/-</sup> cells (Figure S6b). The inactivation of XRCC1 also increased the sensitivity to talazoparib by 10–100 times compared to *wild-type* in both TK6 and MCF-7 cells (Figures 6e–h and S6c). As a result, talazoparib at 1 nM, a clinically relevant concentration (de Bono et al., 2017) significantly killed only *XRCC1*<sup>-/-</sup> cells but not *wild-type*. Collectively, the clinical PARP poisons are synthetic lethal in the absence of XRCC1. XRCC1 is a crucial player in cellular tolerance to clinical PARP poisons.

## 2.7 | The loss of XRCC1 delays SSB repair kinetics even when the PARP1 catalytic activity is inhibited

The synthetic lethality of clinical PARP poisons in *XRCC1*<sup>-/-</sup> cells suggests that XRCC1 suppresses the

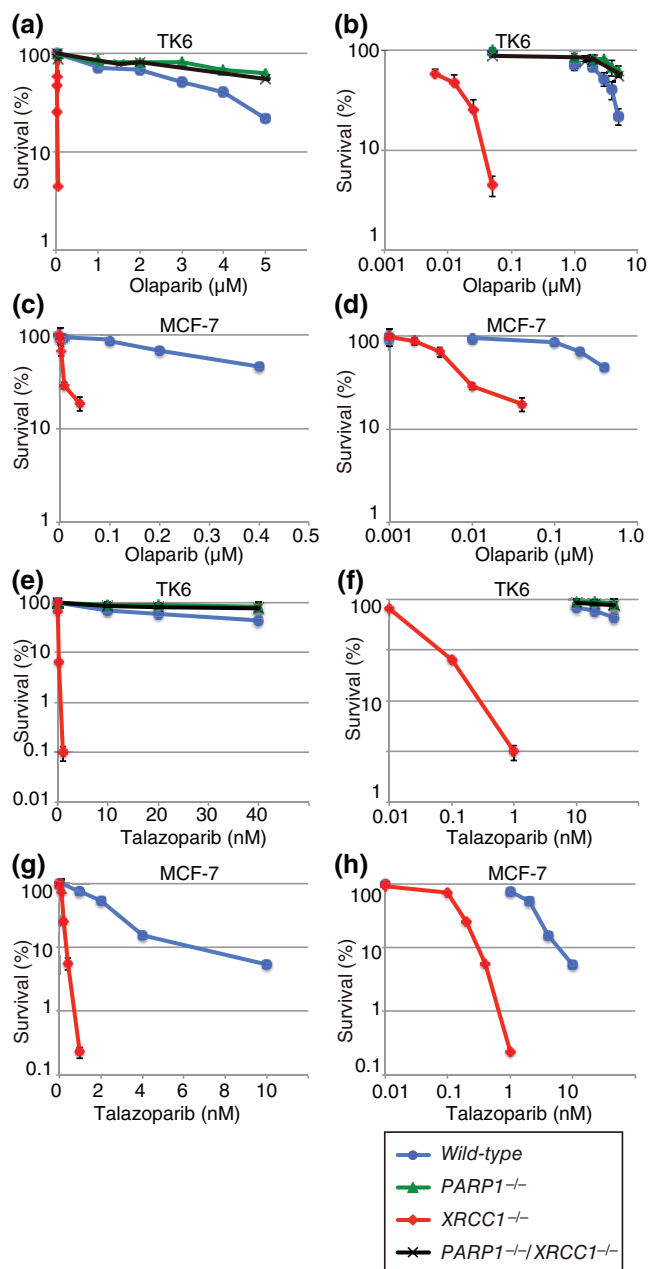


**FIGURE 6** *XRCC1*<sup>-/-</sup> cells are hypersensitive to olaparib and talazoparib. (a–d) The TK6 cells (a,b) and MCF-7 cells (c,d) with indicated genotypes were assessed for sensitivity to olaparib. TK6 or MCF-7 cells were cultured in methylcellulose medium containing olaparib for 14 days. The drug dose is shown on the x-axis on a linear scale (a,c) or on a logarithmic scale (b,d), and the percentage of colony survival is displayed on the y-axis on a logarithmic scale. Error bars represent the SD from three independent experiments. (e–h) The TK6 cells (e,f) and MCF-7 cells (g,h) with indicated genotypes were assessed for sensitivity to talazoparib. TK6 or MCF-7 cells were cultured in methylcellulose medium containing talazoparib for 14 days. The drug dose is shown on the x-axis on a linear scale (e,g) or on a logarithmic scale (f,h), and the percentage of colony survival is displayed on the y-axis on a logarithmic scale. Error bars represent the SD from three independent experiments

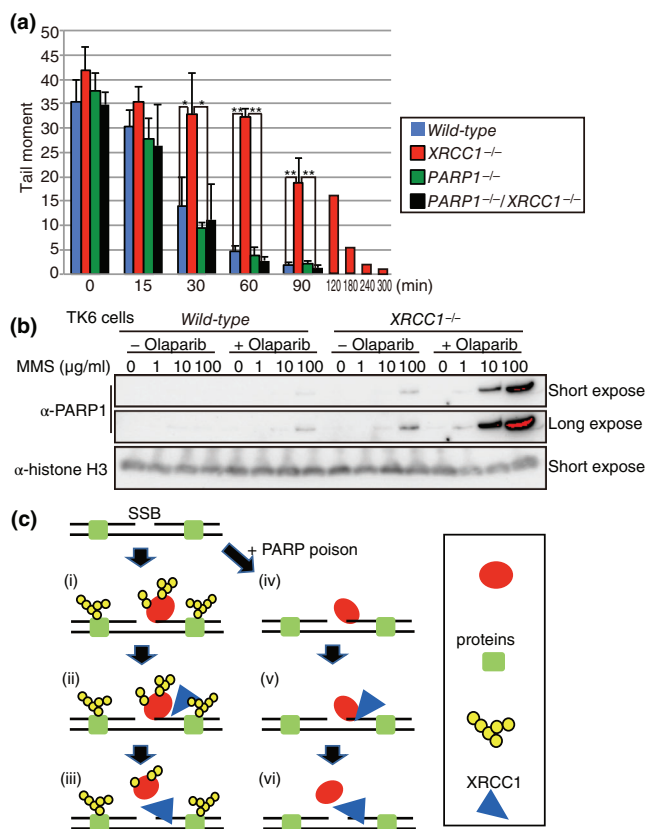


**FIGURE 7** XRCC1 suppresses PARP1 trapping independently of PARP1 activity. (a) Alkaline-comet assay to measure the repair kinetics of SSBs. The indicated TK6 cells were exposed to H<sub>2</sub>O<sub>2</sub> (80 μM) on ice for 30 min, then released into prewarmed culture medium containing olaparib (1 μM) for the indicated times. The median of tail moments for 50 nuclei was measured three times in independent experiments. The means of the tail moments are displayed on the y-axis on a linear scale. Error bars represent SD from three independent experiments. Each data set was presented in Figure S8. The *p*-value was calculated by Student's *t*-test (\**p* < 0.05, \*\**p* < 0.01). (b) Representative western blots probed with the indicated antibodies are presented. The indicated TK6 cells were treated with the indicated concentrations of MMS in the absence or presence olaparib (10 μM) for 1 h. The header indicates cell genotype and the concentrations of MMS treated. (c) XRCC1 prevents PARP1 trapping at SSBs by two mechanisms (i–iii and iv–vi). PARP1 is recruited to SSBs (i, iv) and PARylates chromatin proteins and itself (auto-PARylation) (i) when PARP inhibitors are absent. XRCC1 interacts with PAR (ii) and provides docking sites to BER effector proteins (Figure S2). XRCC1 suppresses excessive PARylation through an unknown mechanism (ii), maintains the level of NAD<sup>+</sup> and auto-PARylation, and facilitates the release of PARP1 from SSBs (iii). XRCC1 is also recruited to SSBs even in the presence of PARP poisons (v) and inhibits the formation of toxic PARP1/SSB complexes independently of the catalytic activity of PARP1 (vi). This inhibition mechanism can prevent the excessive PARylation when PARP poisons are absent (ii). The loss of XRCC1 causes the depletion of NAD<sup>+</sup>, interferes with both auto-PARylation and the release of PARP1, and further decreases the level of NAD<sup>+</sup> in cells in the absence of PARP inhibitors. MMS, methyl methanesulfonate; PARP1, poly(ADP ribose) polymerase 1; SSBs, single-strand breaks

formation of toxic PARP1-SSB complexes even in the absence of PARP1 activity. Olaparib of 0.1 μM represses 90% of PARylation (Murai et al., 2012; Murai et al., 2014), and we added 1.0 μM olaparib immediately after the exposure to H<sub>2</sub>O<sub>2</sub> (Figure 3b). This addition delayed the completion of SSB repair from 15 to 90 min in *wild-type* cells and from 30 to 240 min in XRCC1<sup>-/-</sup> cells (compare Figure 3b and Figures 7a and S8c). We concluded that XRCC1 significantly contributes to SSB repair even when PARP1 catalytic activity is suppressed.

We next performed a pulse-exposure to MMS and olaparib for 1 h, comparing *wild-type* and XRCC1<sup>-/-</sup> cells. The addition of olaparib synergistically increased the amount of MMS-induced stable PARP1-SSB complexes in the absence of XRCC1 (Figure 7b), which data agree with the synthetic lethality of clinical PARP poisons in XRCC1<sup>-/-</sup> cells (Figure 6). These data indicate that XRCC1 promotes the resolution of PARP1-SSB complexes even when the PARP1 catalytic activity is inhibited. Collectively, the loss of XRCC1 synergistically increased the sensitivity of PARP poisons (Figure 6), and olaparib enhanced trapped PARP1 delaying SSB repair (Figure 7). These data indicate that XRCC1 significantly promotes the removal of trapped PARP1 independent of its catalytic activity. In conclusion, XRCC1 removes trapped PARP1 independent of its catalytic activity (Figure 7c, iv–iv) and also by inhibiting its excessive catalysis (Figure 7c, i–iii).

### 3 | DISCUSSION

In this study, we uncovered the significant toxic effect of PARP1 on the repair of base damage induced by TMZ, carmustine, and lomustine (Figures 2 and S7). This endogenous poison activity of PARP1 has been previously unappreciated because XRCC1 completely prevents it (Figures 2 and S7). These results with the clinical alkylating agents agree with the analysis of MMS-treated XRCC1<sup>-/-</sup> and PARP1<sup>-/-</sup>/XRCC1<sup>-/-</sup> RPE and TK6 cells (Demin et al., 2021). We also demonstrated the synthetic lethality between the clinical PARP poisons and the XRCC1 inactivation (Figure 6), which is in sharp contrast with virtually no effect of KU0058948 on the ‘trapping’ of PARP1 in the absence of XRCC1 (Demin et al., 2021). The inhibition of the PARP1 trapping by XRCC1 promotes SSB repair (Figure 3), presumably by allowing SSB repair factors access to SSBs. In summary, our previous work (Demin et al., 2021) and the current study revealed the endogenous poison activity of PARP1 and the complete suppression of the poison activity by XRCC1. This suppression significantly increases cellular tolerance to TMZ, carmustine, lomustine, and the clinical PARP poisons.



It has been believed that XRCC1's key role in BER is to recruit the SSB repair effectors, including aprataxin, LIG3, PNKP, and POL $\beta$ , to unrepaired SSBs (Ali et al., 2009; Caldecott et al., 1994; Cuneo & London, 2010; Iles et al., 2007; Kubota et al., 1996; Marintchev et al., 1999) (reviewed in Caldecott, 2020). However, the inactivation of PARP1 in *XRCC1*<sup>-/-</sup> cells dramatically increases their tolerance to TMZ (Figure 2), indicating that the role of XRCC1 in recruiting SSB repair factors does not explain the very severe phenotype of *XRCC1*<sup>-/-</sup> cells. We demonstrated that XRCC1 promotes BER by inhibiting the endogenous poison activity of PARP1 during exposure to the clinical alkylating drugs. *PARP1*<sup>-/-</sup>/*XRCC1*<sup>-/-</sup> MCF-7 cells showed only modest sensitivity to TMZ, carmustine, and lomustine (Figures 2b and Figure S4), as *PARP1*<sup>-/-</sup>/*XRCC1*<sup>-/-</sup> RPE cells exhibit mild MMS sensitivity (Demin et al., 2021). Collectively, XRCC1 is dispensable for BER of base damage generated by these anti-cancer alkylating drugs in the absence of PARP1.

XRCC1 suppresses the PARP1 trapping through two mechanisms (Figure 7c, i–iii and iv–vi). First, our previous study (Demin et al., 2021) and the present one indicated that XRCC1 maintains auto-PARYlation (Figure 5a), which facilitates the release of PARP1 from unrepaired SSBs (Satoh & Lindahl, 1992), by suppressing both the excessive catalysis of PARP1 at SSBs and the resulting depletion of cellular NAD<sup>+</sup> (Figure 5b). It is unclear how XRCC1 suppresses the excessive activation (Figure 7c, iii). Second, the current study uncovered the synthetic lethality of the *XRCC1*<sup>-/-</sup> mutation and the clinical PARP poisons (Figure 6), suggesting that XRCC1 prevents the PARP1 trapping even when PARP poisons inhibit the auto-PARYlation. This idea is verified by the data that the loss of XRCC1 significantly delayed SSB repair and synergistically increased the number of PARP1/SSB complexes in the presence of olaparib (Figure 7a,b). Thus, XRCC1 is efficiently recruited to unrepaired SSBs without PARYlation (Figure 7c, v) and significantly contributes to SSB repair by inhibiting the trapping of PARP1 at SSBs (Figure 7c, vi). A crucial future question is how XRCC1 prevents the PARP1 trapping independent of its catalytic activity (Figure 7c, iv–vi). A recent report suggested PIAS4-mediated SUMOylation followed by RNF4-mediated ubiquitination of PARP1 removes trapped PARP1 in the absence of its auto-PARYlation (Krastev et al., 2022). XRCC1 plays a more important role in removing trapped PARP1 since the loss of XRCC1 increased the olaparib sensitivity more significantly than that of PIAS4 and RNF4 (Figure 1b). The first and second mechanisms (Figure 7c, i–iii, iv–vi) can collaboratively exacerbate the PARP1 trap. The lack of the catalysis-independent mechanism (Figure 7c, iv–vi) may account for the abnormal PARP1 trapping and the over-catalysis of PARP1 during treatment

of *XRCC1*<sup>-/-</sup> cells with TMZ alone. The following depletion of NAD<sup>+</sup> suppresses auto-PARYlation (Figure 5), leading to the prominent accumulation of toxic PARP1-SSB complexes in *XRCC1*<sup>-/-</sup> cells.

A question is whether or not XRCC1 suppresses the trapping of PARP2, which has overlapping roles with PARP1 (Hanzlikova et al., 2016). Clinical PARP inhibitors cause the trapping of both PARP1 and PARP2 (Murai et al., 2012; Verma et al., 2021). In agreement with the PARP2 trapping, the addition of olaparib delayed the SSB repair of *PARP1*<sup>-/-</sup> and *PARP1*<sup>-/-</sup>/*XRCC1*<sup>-/-</sup> cells by 45 min (compare Figures 3b and 7a). Nonetheless, the very similar sensitivities between *PARP1*<sup>-/-</sup> and *PARP1*<sup>-/-</sup>/*XRCC1*<sup>-/-</sup> cells to TMZ (Figure 2), MMS (Demin et al., 2021), and the clinical PARP poisons (Figure 6) suggest that the PARP2 trapping has no detectable impact on their cytotoxicity. Essentially the same SSB repair kinetics between *PARP1*<sup>-/-</sup> and *PARP1*<sup>-/-</sup>/*XRCC1*<sup>-/-</sup> cells in the presence of olaparib indicated that XRCC1 may not prevent the trapping of PARP2.

We showed that the loss of XRCC1 causes PARP1 to exert its intrinsic poisoning activity, leading to the rapid NAD<sup>+</sup> depletion during treatment with TMZ (Figure 5b). NAD<sup>+</sup> depletion is seen in various diseases, including the postischemic injury of the heart, brain, liver, and kidney, neurodegeneration, and cancer (Adamowicz et al., 2021; Gujar et al., 2016; Hoch et al., 2017; Pieper et al., 2000). NAD<sup>+</sup> depletion by its biosynthesis blockade is used to treat cancers and interferes with BER of TMZ-induced base damage (Goellner et al., 2011; Touat et al., 2018). Inhibitors of poly(ADP-ribose) glycohydrolase also deplete NAD<sup>+</sup> and exacerbate replication stress of cancer cells (reviewed in Hanzlikova & Caldecott, 2019; Slade, 2020). Our discovery of PARP1's intrinsic poisoning activity will provide an insight into the molecular mechanism underlying the dysregulation of this activity caused by the loss of XRCC1 and clinical PARP poisons. The mechanism for the dysregulation is an important future question because excessive PARP1 catalysis and resulting NAD<sup>+</sup> depletion have a profound impact on the viability of cancer cells.

## 4 | EXPERIMENTAL PROCEDURES

### 4.1 | Cell culture, measurement of cellular sensitivity, and measurement of chromosome aberrations

MCF-7 and TK6 cells were obtained from JCRB Cell Bank (<https://cellbank.nibiohn.go.jp/english/>). These cells were

cultured as described previously (Sasanuma et al., 2018; Tsuda, Terada, et al., 2017). To measure sensitivity to alkylating drugs in TK6, we employed a methylcellulose colony-formation assay, as described previously (Ooka et al., 2016), with slight modifications. Briefly, TK6 cells were treated with alkylating reagents (TMZ, carmustine, and lomustine) for 24 h in medium and seeded in a drug-free medium containing 1.5% methylcellulose then cultured at 37°C for 14 days. MCF-7 cells were similarly treated with alkylating reagents for 24 h in medium, and then the treated cells were further cultured in medium without methylcellulose for 14 days. To measure sensitivity to olaparib or talazoparib, we seeded cells in a medium containing olaparib or talazoparib, cultured them for 14 days, and counted the number of colonies. To measure cellular sensitivity to MMS in TK6 cells, we employed a liquid-culture cell survival assay as previously described (Hirota et al., 2015; Hirota et al., 2016).

#### 4.2 | Generation of *PARP1*<sup>-/-</sup> TK6 cells

*PARP1* was disrupted with KO constructs prepared using primers 5'-GCGAATTGGGTACCGGGCCTGGGGAGTAGTGCTTTGTTT-3' and 5'-CTGGGCTCGAGGGGGGCCCTGGAGAATCAAACAGACAG-3' for the left arm and 5'-TGGGAAGCTTGTCGACTTAAGTAAGATCTTGGGGCCAG-3' and 5'-CACTAGTAGGCGCGCCTTAACTTAAATTCCAAATGGCTGG-3' for the right arm. The PCR-amplified left and right arms were inserted in marker-gene plasmids (above described *DT-ApA/NEO<sup>R</sup>*-based plasmids) digested with *ApaI* and *AflII* using the GeneArt Seamless Cloning & Gibson Assembly system (Thermo Fisher Scientific, Pittsburgh, PA) to KO construct. The resultant KO plasmids express diphtheria toxin from outside of the homologous arms to suppress random integration events. The CRISPR expression vector for the CRISPR-Cas9 system was designed to recognize 5'-GAAGTACGTGCAAGGGGTGTATGG-3' (Figure S1). The loss of the *PARP1* expression was confirmed by western blot using antibodies, anti-PARP antibody (Santa Cruz Biotechnology, sc-8007), and anti-histone H3 antibody (Abcam, ab1791) for the loading control.

#### 4.3 | Disruption of *PARP1* and *XRCC1* gene in MCF-7 cells

*PARP1* and *XRCC1* genes were disrupted with the same knockout constructs used for the gene disruption in TK6 cells (Demin et al., 2021; Saha et al., 2020).

#### 4.4 | Isolation of chromatin-bound fractions from TK6 and MCF-7 cells

Chromatin-bound fraction samples were prepared as described previously (Ooka et al., 2018). Briefly, we harvested  $5 \times 10^6$  TK6 or MCF-7 cells and isolated the chromatin-bound fraction from TK6 cells using a subcellular protein fractionation kit for cultured cells (Thermo Fisher Scientific). PARP1 was detected using an anti-PARP antibody (Santa Cruz Biotechnology, sc-8007). Histone was probed as a loading control using an anti-histone H3 antibody (Abcam, ab1791).

#### 4.5 | Alkaline comet assay

TK6 cells were treated with 80  $\mu$ M H<sub>2</sub>O<sub>2</sub> on ice for 30 min and subsequently released in a drug-free, prewarmed culture medium. For the measurement of TMZ-induced SSBs, cells were pulse-exposed to the complete medium containing 0, 150, and 450  $\mu$ M of TMZ for 37°C for 60 min. We performed alkaline-comet and single-cell gel electrophoresis assays as described previously (Tsuda, Cho, et al., 2017). Electrophoresis was carried out by applying 25 volts at 4°C for 50 min using a submarine gel electrophoresis machine (Cat. NB-1012, Nihon Eido Co. Ltd.) filled with 1850 ml running buffer (0.3 M NaOH, 1 mM EDTA). A Comet Analysis System was used to quantify the comet tails (Comet analyzer, Youworks Co. Ltd). We scored over 100 cells per sample.

#### 4.6 | Determination of intracellular NAD<sup>+</sup> concentration

The cellular NAD<sup>+</sup> level was determined by the enzyme cycling assay as previously described (Nakamura et al., 2003). Briefly, exponentially growing culture was diluted to  $1 \times 10^5$  cells/ml and incubated with TMZ (1 mM) for indicated time. A value of 0.5 mL of culture was harvested and the cellular NAD<sup>+</sup> concentration were measured by its reduction to a yellow colored formazan dye using cell counting kit-8 (Dojindo Molecular Technology, Kumamoto, Japan) which consisted of a water-soluble 2-(2-methoxy-4-nitrophenyl)-3-(4-nitrophenyl)-5-(2,4-disulphophenyl)-2H-tetrazolium monosodium salt (WST-8, 5 mM) and 1-methoxy-5-methylphenazinium methylsulfate (0.2 mM) as an electron mediator tetrazolium salt.

## 4.7 | The PARylation assay

A value of  $5 \times 10^6$  of TK6 cells were boiled in standard sodium dodecyl sulfate (SDS) sample buffer for 5 min, and the resultant total protein samples were analyzed by western blot with anti-PAR polyclonal antibody (4336-BPC-100, Trevigen)

### ACKNOWLEDGMENTS

The authors thank the TK6 Mutants Consortium (<http://www.nihs.go.jp/dgm/tk6.html>) for their critical help in establishing methods for gene-disruption using the TK6 cell line. This work was partly supported by the Network-type Joint Usage/Research Center for Radiation Disaster Medical Science of Hiroshima University, Nagasaki University, and Fukushima Medical University.

### CONFLICT OF INTEREST

The authors declare no potential conflict of interest.

### AUTHOR CONTRIBUTIONS

*Conceived and designed the experiments:* Kouji Hirota and Shunichi Takeda. *Performed the experiments:* Kouji Hirota, Masato Ooka, Naoto Shimizu, Kousei Yamada, Masataka Tsuda, Mahmoud Abdelghany Ibrahim, Shintaro Yamada, and Hiroyuki Sasanuma. *Wrote the paper:* Kouji Hirota and Shunichi Takeda.

### ORCID

Kouji Hirota  <https://orcid.org/0000-0003-1676-979X>

### REFERENCES

- Adamowicz, M., Hailstone, R., Demin, A. A., Komulainen, E., Hanzlikova, H., Brazina, J., Gautam, A., Wells, S. E., & Caldecott, K. W. (2021). XRCC1 protects transcription from toxic PARP1 activity during DNA base excision repair. *Nature Cell Biology*, *23*, 1287–1298.
- Ahel, D., Horejsi, Z., Wiechens, N., Polo, S. E., Garcia-Wilson, E., Ahel, I., Flynn, H., Skehel, M., West, S. C., Jackson, S. P., Owen-Hughes, T., & Boulton, S. J. (2009). Poly(ADP-ribose)-dependent regulation of DNA repair by the chromatin remodeling enzyme ALC1. *Science*, *325*, 1240–1243.
- Ali, A. A., Jukes, R. M., Pearl, L. H., & Oliver, A. W. (2009). Specific recognition of a multiply phosphorylated motif in the DNA repair scaffold XRCC1 by the FHA domain of human PNK. *Nucleic Acids Research*, *37*, 1701–1712.
- Barnes, D. E., & Lindahl, T. (2004). Repair and genetic consequences of endogenous DNA base damage in mammalian cells. *Annual Review of Genetics*, *38*, 445–476.
- Blessing, C., Mandemaker, I. K., Gonzalez-Leal, C., Preisser, J., Schomburg, A., & Ladurner, A. G. (2020). The oncogenic helicase ALC1 regulates PARP inhibitor potency by trapping PARP2 at DNA breaks. *Molecular Cell*, *80*, 862–875. e866.
- Breslin, C., Clements, P. M., El-Khamisy, S. F., Petermann, E., Iles, N., & Caldecott, K. W. (2006). Measurement of chromosomal DNA single-strand breaks and replication fork progression rates. *Methods in Enzymology*, *409*, 410–425.
- Bryant, H. E., Schultz, N., Thomas, H. D., Parker, K. M., Flower, D., Lopez, E., Kyle, S., Meuth, M., Curtin, N. J., & Helleday, T. (2005). Specific killing of BRCA2-deficient tumours with inhibitors of poly(ADP-ribose) polymerase. *Nature*, *434*, 913–917.
- Caldecott, K. W. (2003). XRCC1 and DNA strand break repair. *DNA Repair (Amst)*, *2*, 955–969.
- Caldecott, K. W. (2008). Single-strand break repair and genetic disease. *Nature Reviews. Genetics*, *9*, 619–631.
- Caldecott, K. W. (2014). Protein ADP-ribosylation and the cellular response to DNA strand breaks. *DNA Repair (Amst)*, *19*, 108–113.
- Caldecott, K. W. (2020). Mammalian DNA base excision repair: Dancing in the moonlight. *DNA Repair (Amst)*, *93*, 102921.
- Caldecott, K. W., Aoufouchi, S., Johnson, P., & Shall, S. (1996). XRCC1 polypeptide interacts with DNA polymerase beta and possibly poly(ADP-ribose) polymerase, and DNA ligase III is a novel molecular “nick-sensor” in vitro. *Nucleic Acids Research*, *24*, 4387–4394.
- Caldecott, K. W., McKeown, C. K., Tucker, J. D., Ljungquist, S., & Thompson, L. H. (1994). An interaction between the mammalian DNA repair protein XRCC1 and DNA ligase III. *Molecular and Cellular Biology*, *14*, 68–76.
- Caldecott, K. W., Tucker, J. D., Stanker, L. H., & Thompson, L. H. (1995). Characterization of the XRCC1-DNA ligase III complex in vitro and its absence from mutant hamster cells. *Nucleic Acids Research*, *23*, 4836–4843.
- Cistulli, C., Lavrik, O. I., Prasad, R., Hou, E., & Wilson, S. H. (2004). AP endonuclease and poly(ADP-ribose) polymerase-1 interact with the same base excision repair intermediate. *DNA Repair (Amst)*, *3*, 581–591.
- Cuneo, M. J., & London, R. E. (2010). Oxidation state of the XRCC1 N-terminal domain regulates DNA polymerase beta binding affinity. *Proceedings of the National Academy of Sciences of the United States of America*, *107*, 6805–6810.
- Danam, R. P., Howell, S. R., Brent, T. P., & Harris, L. C. (2005). Epigenetic regulation of O6-methylguanine-DNA methyltransferase gene expression by histone acetylation and methyl-CpG binding proteins. *Molecular Cancer Therapeutics*, *4*, 61–69.
- de Bono, J., Ramanathan, R. K., Mina, L., Chugh, R., Glaspy, J., Rafii, S., Kaye, S., Sachdev, J., Heymach, J., Smith, D. C., Henshaw, J. W., Herriott, A., Patterson, M., Curtin, N. J., Byers, L. A., & Wainberg, Z. A. (2017). Phase I, dose-escalation, two-part trial of the PARP inhibitor talazoparib in patients with advanced germline BRCA1/2 mutations and selected sporadic cancers. *Cancer Discovery*, *7*, 620–629.
- Demin, A. A., Hirota, K., Tsuda, M., Adamowicz, M., Hailstone, R., Brazina, J., Gittens, W., Kalasova, I., Shao, Z., Zha, S., Sasanuma, H., Hanzlikova, H., Takeda, S., & Caldecott, K. W. (2021). XRCC1 prevents toxic PARP1 trapping during DNA base excision repair. *Molecular Cell*, *81*, 3018–3030.e3015.
- Desai, K., Hubben, A., & Ahluwalia, M. (2019). The role of checkpoint inhibitors in glioblastoma. *Targeted Oncology*, *14*, 375–394.
- Doetsch, P. W., & Cunningham, R. P. (1990). The enzymology of apurinic/aprimidinic endonucleases. *Mutation Research*, *236*, 173–201.

- Doetsch, P. W., Helland, D. E., & Haseltine, W. A. (1986). Mechanism of action of a mammalian DNA repair endonuclease. *Biochemistry*, *25*, 2212–2220.
- El-Khamisy, S. F., Masutani, M., Suzuki, H., & Caldecott, K. W. (2003). A requirement for PARP-1 for the assembly or stability of XRCC1 nuclear foci at sites of oxidative DNA damage. *Nucleic Acids Research*, *31*, 5526–5533.
- Esteller, M., Garcia-Foncillas, J., Andion, E., Goodman, S. N., Hidalgo, O. F., Vanaclocha, V., Baylin, S. B., & Herman, J. G. (2000). Inactivation of the DNA-repair gene MGMT and the clinical response of gliomas to alkylating agents. *The New England Journal of Medicine*, *343*, 1350–1354.
- Farmer, H., McCabe, N., Lord, C. J., Tutt, A. N., Johnson, D. A., Richardson, T. B., Santarosa, M., Dillon, K. J., Hickson, I., Knights, C., Martin, N. M., Jackson, S. P., Smith, G. C., & Ashworth, A. (2005). Targeting the DNA repair defect in BRCA mutant cells as a therapeutic strategy. *Nature*, *434*, 917–921.
- Fong, P. C., Boss, D. S., Yap, T. A., Tutt, A., Wu, P., Mergui-Roelvink, M., Mortimer, P., Swaisland, H., Lau, A., O'Connor, M. J., Ashworth, A., Carmichael, J., Kaye, S. B., Schellens, J. H., & de Bono, J. S. (2009). Inhibition of poly(ADP-ribose) polymerase in tumors from BRCA mutation carriers. *The New England Journal of Medicine*, *361*, 123–134.
- Goellner, E. M., Grimme, B., Brown, A. R., Lin, Y. C., Wang, X. H., Sugrue, K. F., Mitchell, L., Trivedi, R. N., Tang, J. B., & Sobol, R. W. (2011). Overcoming temozolomide resistance in glioblastoma via dual inhibition of NAD<sup>+</sup> biosynthesis and base excision repair. *Cancer Research*, *71*, 2308–2317.
- Gujar, A. D., Le, S., Mao, D. D., Dadey, D. Y., Turski, A., Sasaki, Y., Aum, D., Luo, J., Dahiya, S., Yuan, L., Rich, K. M., Milbrandt, J., Hallahan, D. E., Yano, H., Tran, D. D., & Kim, A. H. (2016). An NAD<sup>+</sup>-dependent transcriptional program governs self-renewal and radiation resistance in glioblastoma. *Proceedings of the National Academy of Sciences of the United States of America*, *113*, E8247–E8256.
- Hanzlikova, H., & Caldecott, K. W. (2019). Perspectives on PARPs in S phase. *Trends in Genetics*, *35*, 412–422.
- Hanzlikova, H., Gittens, W., Krejciikova, K., Zeng, Z., & Caldecott, K. W. (2016). Overlapping roles for PARP1 and PARP2 in the recruitment of endogenous XRCC1 and PNKP into oxidized chromatin. *Nucleic Acids Research*, *45*, gkw1246–gkw2557.
- Hewitt, G., Borel, V., Segura-Bayona, S., Takaki, T., Ruis, P., Bellelli, R., Lehmann, L. C., Sommerova, L., Vancevska, A., Tomas-Loba, A., Zhu, K., Cooper, C., Fugger, K., Patel, H., Goldstone, R., Schneider-Luftman, D., Herbert, E., Stamp, G., Brough, R., ... Boulton, S. J. (2021). Defective ALC1 nucleosome remodeling confers PARPi sensitization and synthetic lethality with HRD. *Molecular Cell*, *81*, 767–783.e711.
- Hirota, K., Tsuda, M., Mohiuddin, Tsurimoto, T., Cohen, I. S., Livneh, Z., Kobayashi, K., Narita, T., Nishihara, K., Murai, J., Iwai, S., Guilbaud, G., Sale, J. E., & Takeda, S. (2016). In vivo evidence for translesion synthesis by the replicative DNA polymerase delta. *Nucleic Acids Research*, *44*, 7242–7250.
- Hirota, K., Yoshikiyo, K., Guilbaud, G., Tsurimoto, T., Murai, J., Tsuda, M., Phillips, L. G., Narita, T., Nishihara, K., Kobayashi, K., Yamada, K., Nakamura, J., Pommier, Y., Lehmann, A., Sale, J. E., & Takeda, S. (2015). The POLD3 subunit of DNA polymerase delta can promote translesion synthesis independently of DNA polymerase zeta. *Nucleic Acids Research*, *43*, 1671–1683.
- Hoch, N. C., Hanzlikova, H., Rulten, S. L., Tétreault, M., Komulainen, E., Ju, L., Hornyak, P., Zeng, Z., Gittens, W., Rey, S. A., Staras, K., Mancini, G. M. S., McKinnon, P. J., Wang, Z.-Q., Wagner, J. D., Care4Rare Canada Consortium, Yoon, G., & Caldecott, K. W. (2017). XRCC1 mutation is associated with PARP1 hyperactivation and cerebellar ataxia. *Nature*, *541*, 87–91.
- Horton, J. K., Stefanick, D. F., Prasad, R., Gassman, N. R., Kedar, P. S., & Wilson, S. H. (2014). Base excision repair defects invoke hypersensitivity to PARP inhibition. *Molecular Cancer Research*, *12*, 1128–1139.
- Horton, J. K., Watson, M., Stefanick, D. F., Shaughnessy, D. T., Taylor, J. A., & Wilson, S. H. (2008). XRCC1 and DNA polymerase beta in cellular protection against cytotoxic DNA single-strand breaks. *Cell Research*, *18*, 48–63.
- Horton, J. K., & Wilson, S. H. (2013). Predicting enhanced cell killing through PARP inhibition. *Molecular Cancer Research*, *11*, 13–18.
- Iles, N., Rulten, S., El-Khamisy, S. F., & Caldecott, K. W. (2007). APLF (C2orf13) is a novel human protein involved in the cellular response to chromosomal DNA strand breaks. *Molecular and Cellular Biology*, *27*, 3793–3803.
- Juhász, S., Smith, R., Schauer, T., Spekhardt, D., Mamar, H., Zentout, S., Chapuis, C., Huet, S., & Timinszky, G. (2020). The chromatin remodeler ALC1 underlies resistance to PARP inhibitor treatment. *Science Advances*, *6*(51), eabb8626.
- Kaina, B., & Christmann, M. (2019). DNA repair in personalized brain cancer therapy with temozolomide and nitrosoureas. *DNA Repair (Amst)*, *78*, 128–141.
- Kaina, B., Christmann, M., Naumann, S., & Roos, W. P. (2007). MGMT: Key node in the battle against genotoxicity, carcinogenicity and apoptosis induced by alkylating agents. *DNA Repair (Amst)*, *6*, 1079–1099.
- Krastev, D. B., Li, S., Sun, Y., Wicks, A. J., Hoslett, G., Weekes, D., Badder, L. M., Knight, E. G., Marlow, R., Pardo, M. C., Yu, L., Talele, T. T., Bartek, J., Choudhary, J. S., Pommier, Y., Pettitt, S. J., Tutt, A. N. J., Ramadan, K., & Lord, C. J. (2022). The ubiquitin-dependent ATPase p97 removes cytotoxic trapped PARP1 from chromatin. *Nature Cell Biology*, *24*, 62–73.
- Kubota, Y., Nash, R. A., Klungland, A., Schar, P., Barnes, D. E., & Lindahl, T. (1996). Reconstitution of DNA base excision-repair with purified human proteins: Interaction between DNA polymerase beta and the XRCC1 protein. *The EMBO Journal*, *15*, 6662–6670.
- Marintchev, A., Mullen, M. A., Maciejewski, M. W., Pan, B., Gryk, M. R., & Mullen, G. P. (1999). Solution structure of the single-strand break repair protein XRCC1 N-terminal domain. *Nature Structural Biology*, *6*, 884–893.
- Murai, J., Huang, S. Y., Das, B. B., Renaud, A., Zhang, Y., Doroshow, J. H., Ji, J., Takeda, S., & Pommier, Y. (2012). Trapping of PARP1 and PARP2 by clinical PARP inhibitors. *Cancer Research*, *72*, 5588–5599.
- Murai, J., Huang, S. Y., Renaud, A., Zhang, Y., Ji, J., Takeda, S., Morris, J., Teicher, B., Doroshow, J. H., & Pommier, Y. (2014). Stereospecific PARP trapping by BMN 673 and comparison



- with olaparib and rucaparib. *Molecular Cancer Therapeutics*, *13*, 433–443.
- Nakamura, J., Asakura, S., Hester, S.D., de Murcia, G., Caldecott, K.W. & Swenberg, J.A. (2003) Quantitation of intracellular NAD(P)H can monitor an imbalance of DNA single strand break repair in base excision repair deficient cells in real time. *Nucleic Acids Research* *31*, e104, 104e, 1104.
- Okano, S., Lan, L., Caldecott, K. W., Mori, T., & Yasui, A. (2003). Spatial and temporal cellular responses to single-strand breaks in human cells. *Molecular and Cellular Biology*, *23*, 3974–3981.
- Olivieri, M., Cho, T., Álvarez-Quilón, A., Li, K., Schellenberg, M. J., Zimmermann, M., Hustedt, N., Rossi, S. E., Adam, S., Melo, H., Heijink, A. M., Sastre-Moreno, G., Moatti, N., Szilard, R. K., McEwan, A., Ling, A. K., Serrano-Benitez, A., Ubhi, T., Feng, S., ... Durocher, D. (2020). A genetic map of the response to DNA damage in human cells. *Cell*, *182*, 481–496.e421.
- Ooka, M., Abe, T., Cho, K., Koike, K., Takeda, S., & Hirota, K. (2018). Chromatin remodeler ALC1 prevents replication-fork collapse by slowing fork progression. *PLoS One*, *13*, e0192421.
- Ooka, M., Kobayashi, K., Abe, T., Akiyama, K., Hada, M., Takeda, S., & Hirota, K. (2016). Determination of genotoxic potential by comparison of structurally related Azo dyes using DNA repair-deficient DT40 mutant panels. *Chemosphere*, *164*, 106–112.
- Penketh, P. G., Shyam, K., & Sartorelli, A. C. (2000). Comparison of DNA lesions produced by tumor-inhibitory 1,2-bis(sulfonyl)hydrazines and chloroethylnitrosoureas. *Biochemical Pharmacology*, *59*, 283–291.
- Pieper, A. A., Walles, T., Wei, G., Clements, E. E., Verma, A., Snyder, S. H., & Zweier, J. L. (2000). Myocardial postischemic injury is reduced by polyADPribose polymerase-1 gene disruption. *Molecular Medicine*, *6*, 271–282.
- Prasad, R., Horton, J. K., Chastain, P. D., 2nd, Gassman, N. R., Freudenthal, B. D., Hou, E. W., & Wilson, S. H. (2014). Suicidal cross-linking of PARP-1 to AP site intermediates in cells undergoing base excision repair. *Nucleic Acids Research*, *42*, 6337–6351.
- Ray Chaudhuri, A., & Nussenzweig, A. (2017). The multifaceted roles of PARP1 in DNA repair and chromatin remodelling. *Nature Reviews. Molecular Cell Biology*, *18*, 610–621.
- Saha, L. K., Wakasugi, M., Akter, S., Prasad, R., Wilson, S. H., Shimizu, N., Sasanuma, H., Huang, S. N., Agama, K., Pommier, Y., Matsunaga, T., Hirota, K., Iwai, S., Nakazawa, Y., Ogi, T., & Takeda, S. (2020). Topoisomerase I-driven repair of UV-induced damage in NER-deficient cells. *Proceedings of the National Academy of Sciences of the United States of America*, *117*, 14412–14420.
- Sasanuma, H., Tsuda, M., Morimoto, S., Saha, L. K., Rahman, M. M., Kiyooka, Y., Fujiike, H., Cherniack, A. D., Itou, J., Callen Moreau, E., Toi, M., Nakada, S., Tanaka, H., Tsutsui, K., Yamada, S., Nussenzweig, A., & Takeda, S. (2018). BRCA1 ensures genome integrity by eliminating estrogen-induced pathological topoisomerase II-DNA complexes. *Proceedings of the National Academy of Sciences of the United States of America*, *115*, E10642–E10651.
- Satoh, M. S., & Lindahl, T. (1992). Role of poly(ADP-ribose) formation in DNA repair. *Nature*, *356*, 356–358.
- Shen, Y., Rehman, F. L., Feng, Y., Boshuizen, J., Bajrami, I., Elliott, R., Wang, B., Lord, C. J., Post, L. E., & Ashworth, A. (2013). BMN 673, a novel and highly potent PARP1/2 inhibitor for the treatment of human cancers with DNA repair deficiency. *Clinical Cancer Research*, *19*, 5003–5015.
- Slade, D. (2020). PARP and PARG inhibitors in cancer treatment. *Genes & Development*, *34*, 360–394.
- Stupp, R., Lukas, R. V., & Hegi, M. E. (2019). Improving survival in molecularly selected glioblastoma. *Lancet*, *393*, 615–617.
- Sun, K., Mikule, K., Wang, Z., Poon, G., Vaidyanathan, A., Smith, G., Zhang, Z. Y., Hanke, J., Ramaswamy, S., & Wang, J. (2018). A comparative pharmacokinetic study of PARP inhibitors demonstrates favorable properties for niraparib efficacy in preclinical tumor models. *Oncotarget*, *9*, 37080–37096.
- Tebbs, R. S., Flannery, M. L., Meneses, J. J., Hartmann, A., Tucker, J. D., Thompson, L. H., Cleaver, J. E., & Pedersen, R. A. (1999). Requirement for the Xrcc1 DNA base excision repair gene during early mouse development. *Developmental Biology*, *208*, 513–529.
- Tebbs, R. S., Thompson, L. H., & Cleaver, J. E. (2003). Rescue of Xrcc1 knockout mouse embryo lethality by transgene-complementation. *DNA Repair (Amst)*, *2*, 1405–1417.
- Thomas, A., Tanaka, M., Trepel, J., Reinhold, W. C., Rajapakse, V. N., & Pommier, Y. (2017). Temozolomide in the era of precision medicine. *Cancer Research*, *77*, 823–826.
- Touat, M., Sourisseau, T., Dorvault, N., Chabanon, R. M., Garrido, M., Morel, D., Krastev, D. B., Bigot, L., Adam, J., Frankum, J. R., Durand, S., Pontoizeau, C., Souquère, S., Kuo, M. S., Sauvaigo, S., Mardakheh, F., Sarasin, A., Olausson, K. A., Friboulet, L., ... Postel-Vinay, S. (2018). DNA repair deficiency sensitizes lung cancer cells to NAD<sup>+</sup> biosynthesis blockade. *The Journal of Clinical Investigation*, *128*, 1671–1687.
- Tsuda, M., Cho, K., Ooka, M., Shimizu, N., Watanabe, R., Yasui, A., Nakazawa, Y., Ogi, T., Harada, H., Agama, K., Nakamura, J., Asada, R., Fujiike, H., Sakuma, T., Yamamoto, T., Murai, J., Hiraoka, M., Koike, K., Pommier, Y., ... Hirota, K. (2017). ALC1/CHD1L, a chromatin-remodeling enzyme, is required for efficient base excision repair. *PLoS One*, *12*, e0188320.
- Tsuda, M., Terada, K., Ooka, M., Kobayashi, K., Sasanuma, H., Fujisawa, R., Tsurimoto, T., Yamamoto, J., Iwai, S., Kadoda, K., Akagawa, R., Huang, S. Y. N., Pommier, Y., Sale, J. E., Takeda, S., & Hirota, K. (2017). The dominant role of proofreading exonuclease activity of replicative polymerase epsilon in cellular tolerance to cytarabine (Ara-C). *Oncotarget*, *8*, 33457–33474.
- Tubbs, A., & Nussenzweig, A. (2017). Endogenous DNA damage as a source of genomic instability in cancer. *Cell*, *168*, 644–656.
- Verma, P., Zhou, Y., Cao, Z., Deraska, P. V., Deb, M., Arai, E., Li, W., Shao, Y., Puentes, L., Li, Y., Patankar, S., Mach, R. H., Faryabi, R. B., Shi, J., & Greenberg, R. A. (2021). ALC1 links chromatin accessibility to PARP inhibitor response in homologous recombination-deficient cells. *Nature Cell Biology*, *23*, 160–171.
- Yap, T. A., Plummer, R., Azad, N. S., & Helleday, T. (2019). The DNA damaging revolution: PARP inhibitors and beyond. *American Society of Clinical Oncology Educational Book*, *39*, 185–195.

- Yu, W., Zhang, L., Wei, Q., & Shao, A. (2019). O(6)-Methylguanine-DNA methyltransferase (MGMT): Challenges and new opportunities in glioma chemotherapy. *Frontiers in Oncology*, *9*, 1547.
- Zhang, L. S., Honma, M., Hayashi, M., Suzuki, T., Matsuoka, A., & Sofuni, T. (1995). A comparative study of TK6 human lymphoblastoid and L5178Y mouse lymphoma cell lines in the in vitro micronucleus test. *Mutation Research*, *347*, 105–115.

### SUPPORTING INFORMATION

Additional supporting information may be found in the online version of the article at the publisher's website.

**How to cite this article:** Hirota, K., Ooka, M., Shimizu, N., Yamada, K., Tsuda, M., Ibrahim, M. A., Yamada, S., Sasanuma, H., Masutani, M., & Takeda, S. (2022). XRCC1 counteracts poly(ADP ribose)polymerase (PARP) poisons, olaparib and talazoparib, and a clinical alkylating agent, temozolomide, by promoting the removal of trapped PARP1 from broken DNA. *Genes to Cells*, *27*(5), 331–344. <https://doi.org/10.1111/gtc.12929>